

## Grain-size dependence of thermal properties of nanocrystalline elemental selenium studied by x-ray diffraction

Y. H. Zhao and K. Lu\*

*State Key Laboratory for RSA, Institute of Metal Research, Chinese Academy of Sciences,  
Shenyang 110015, People's Republic of China*

(Received 3 February 1997; revised manuscript received 23 April 1997)

Quantitative x-ray-diffraction measurements in a temperature range 88–325 K were performed on porosity-free nanocrystalline (nc) elemental Se samples with a hcp structure. The nc-Se samples with different grain sizes were synthesized by crystallizing a melt-quenched amorphous-Se solid. Thermal-expansion coefficients (TECs) for the nc-Se samples were determined according to the temperature dependence of the lattice parameters ( $a$  and  $c$ ) and the unit-cell volume ( $V$ ). It was found that at higher temperatures the lattice expands along  $a$  axis but contracts along  $c$  axis. With a reduction of grain size, the linear TECs (both along  $a$  axis and  $c$  axis) increase significantly, resulting in an evident increase in the volume TEC that follows the  $D^{-1}$  rule. The temperature dependence of the mean Debye-Waller parameter (DWP) was measured, from which the static and thermal components of the DWP, as well as the Debye characteristic temperature for the nc-Se samples were obtained. The observed enhancement in the mean DWP can be attributed mainly to the increase of static atomic displacement with a reduction of grain size that follows the  $D^{-1}$  rule. The characteristic temperature for the nc-Se specimens was found to decrease significantly with a refinement of grains. These results suggest larger displacements of the atoms from their ideal lattice locations and more defects in the nc-Se samples with smaller grains. [S0163-1829(97)07045-8]

### I. INTRODUCTION

Investigation on the temperature-dependent properties can provide vital information related to the intrinsic structure characteristics of nanocrystalline (nc) materials. In recent years, thermal properties of nc materials have been extensively investigated in many cases. Comparative studies indicated that heat capacity at constant pressure ( $c_p$ ) of nc Pd and Cu (fcc) made by consolidation of ultrafine particles (UFPs) is much enhanced (as much as 60%) with respect to that of their coarse-grained polycrystalline counterparts and the amorphous solids.<sup>1</sup> In the ball-milled nc-Ru sample, an enhancement in  $c_p$  of about 20% was also reported.<sup>2</sup> Nevertheless, rather small heat capacity enhancements (1–2 %) were observed in porosity-free nc specimens [Ni-P (Ref. 3), Se (Ref. 4), and Ni (Ref. 5)] synthesized by means of crystallization of amorphous solids and electrodeposition, respectively. As to thermal-expansion behaviors for nc materials, different observations have been reported. Dilatometric measurements indicated that the linear thermal-expansion coefficient ( $\alpha_L$ ) of a 7 nm Pd is about 80% higher than that for the coarse-grained polycrystalline Pd (Ref. 6). Birringer and Gleiler<sup>7</sup> found that the thermal-expansion coefficient of a 8 nm Cu is about 1.94 times that for the crystalline sample. However, Eastman and co-workers<sup>8</sup> measured the temperature dependence of the lattice parameter by means of x-ray diffraction (XRD) and found no essential difference in thermal-expansion coefficients between the nc and the coarse-grained Pd samples. The grain-size dependence of the thermal-expansion coefficient in the porosity-free nc Ni-P (Ref. 9) samples indicated an evident enhancement in  $\alpha_L$  compared to that of the coarse-grained sample, but the enhancement does not follow the simple  $D^{-1}$  ( $D$  is the mean

grain size) rule as expected from the two-state model of nc materials.<sup>10</sup>

The Debye-Waller parameter (DWP) consists of a static (temperature-independent) and a thermal (temperature-dependent) component. The thermal DWP reflects the vibrational motion of atoms about their equilibrium lattice sites, while the static DWP is due to any static displacements of atoms from their equilibrium sites caused by defects. Comparative studies indicated that the mean DWPs of nc Pd (Refs. 8 and 11) made by consolidation of UFPs and uncompact powders [Pd (Refs. 12 and 13) Au (Refs. 14 and 15) Cr (Ref. 10) and Pb (Ref. 16)] are much enhanced with decreasing grain size or particle size. It was found that the static DWP is normally increasing significantly with a reduction of grain/particle size, while the temperature-dependent thermal DWP shows no measurable (or very slight<sup>15</sup>) grain-size dependence in nc materials. The enhanced static DWP is normally attributed to the concentrations of defects in grain boundaries and/or free-surface regions.<sup>10</sup> A parameter related to DWP is the characteristic temperature that designates the cohesion of atoms. Reduced Debye temperatures are frequently observed in nanometer-sized metallic powders<sup>15,17</sup> and their compacts.<sup>18,19</sup>

These observations indicate that thermal properties of nc materials differ evidently from those of their conventional coarse-grained counterparts. However, a systematic investigation of the grain-size dependence of these thermal properties in nc materials with a wide grain-size range and a different crystallographic structure (rather than cubic) is seldom reported. Moreover, thermal properties, like other physical and mechanical properties, are strongly related to the structure features (such as porosity, contamination, residual strain, etc.) that are closely related to the preparation and processing of the nc sample. Therefore, it is of significance

TABLE I. A list of the annealing temperature and the resultant mean grain size in the as-crystallized nc-Se samples. The mean grain size was derived from XRD experiments and verified by TEM observations.

Sample	A	B	C	D	E
Annealing temperature (K)	363	384	393	403	453
Mean grain size, $D$ (nm)	$13 \pm 2$	$19 \pm 1$	$21 \pm 2$	$24 \pm 2$	$46 \pm 4$

to study the grain-size dependence of thermal properties in a well-characterized nc material.

In this paper, thermal properties of porosity-free nc element Se (hcp) samples with mean grain sizes of 13–46 nm made by crystallization of amorphous solid were measured by means of x-ray diffraction over a temperature range, 88–325 K. Thermal-expansion coefficients, DWP, and the characteristic temperatures were determined as a function of grain size. These thermal properties and their grain-size dependencies will be analyzed in correlation with the observed microstructure characteristics as reported in our previous paper.<sup>20</sup>

## II. EXPERIMENTAL PROCEDURES

### A. Sample preparation and x-ray-diffraction experiments

The nanocrystalline selenium specimens used in the present work were synthesized by completely crystallizing the melt-quenched amorphous selenium solid, of which the procedure was described in detail in our previous paper.<sup>20</sup> Table I lists the annealing conditions and the mean grain size of the nc-Se specimens to be used in the present work.

The quantitative x-ray-diffraction measurements of the nc-Se samples at different temperatures (88–325 K) were carried out on a Rigaku D/MAX 2400 x-ray diffractometer with a wide angle goniometer. The XRD experiment conditions are the same as in Ref. 20. Only nine single Bragg reflection peaks (100), (101), (200), (201), (210), (211), (113), (104), and (302) of the nc-Se sample were measured in the present work. The temperature with an accuracy of  $\pm 2$  K was calibrated by means of the  $\text{NH}_4\text{NO}_3$  sample in which a hexagonal-to-orthorhombic phase transition occurs at 255 K. The liquid nitrogen was used to cool the sample and a copper-constantan thermocouple was used.

### B. Data analysis

Thermal-expansion coefficients of the nc-Se samples were determined based on the measurement results of lattice parameters and the unit-cell volume at various temperatures. The evaluation of lattice parameters was described in detail in Ref. 20.

For a crystal containing only one kind of atom, the thermal vibration of atoms reduces the intensities of diffraction lines by the Debye-Waller factor,  $\exp(-2M)$ . The observed integrated intensity per unit length along the  $hkl$  diffraction line is given by<sup>21</sup>

$$I_{\text{obs}}(hkl) = SI_{\text{cal}}(hkl)\exp(-2M), \quad (1)$$

where  $I_{\text{cal}}(hkl)$  is the calculated integrated intensity without the Debye-Waller factor and  $S$  is a scale factor. The value

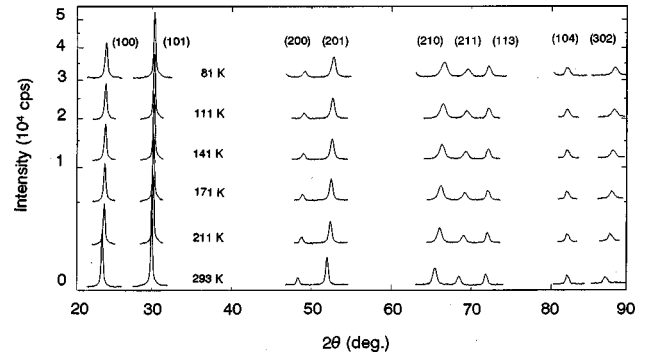


FIG. 1. The x-ray diffraction profiles for the nc-Se sample with a mean grain size of 46 nm at different temperatures (as indicated).

$2M$  is proportional to the square of scattering vector  $4\pi^2(\sin\theta/\lambda)^2$  and is given by<sup>21</sup>

$$2M = 2B(T)(\sin\theta/\lambda)^2, \quad (2)$$

where  $B(T)$  is the Debye-Waller parameter, which is related to the mean-square atomic displacement,  $\langle\mu^2\rangle$ , along the scattering vector by  $B = 8\pi^2\langle\mu^2\rangle$ . From Eqs. (1) and (2), the DWP  $B(T)$  can be obtained at any temperature by

$$\ln[I_{\text{obs}}(hkl)/I_{\text{cal}}(hkl)] = -2B(T)(\sin\theta/\lambda)^2 + \text{const.} \quad (3)$$

The DWP  $B(T)$  contains the contributions from static lattice distortions  $B_S$  that are temperature-independent and from the thermal vibrations of atoms  $B_T$ , i.e.,<sup>21</sup>

$$B(T) = B_S + B_T. \quad (4)$$

For a bulk crystal, the temperature dependence of  $B_T$  is known to be well predicted by the Debye approximation, particularly at low temperatures, and the DWP  $B(T)$  is used to calculate the Debye temperature,  $\Theta_D$ , from the expression<sup>22</sup>

$$B(T) = B_S + 6h^2F(x)/mk_B\Theta_D, \quad (5)$$

where  $m$ ,  $h$ , and  $k_B$  are the atomic mass, the Planck's constant, and the Boltzmann constant, respectively,  $x = \Theta_D/T$  and  $F(x) = \frac{1}{4} + 1/x^2 \int_0^x \xi d\xi / [\exp(\xi) - 1]$ . It is known that the Debye model is normally applicable to cubic crystals. However, for the hexagonal structure of Se as in the present case, we utilized it as an approximation because no existing model is available for the hexagonal structure.

## III. RESULTS AND DISCUSSION

Figure 1 shows the typical x-ray diffraction lines for nc-Se sample *E* at various temperatures. With an increasing temperature, the XRD peaks shift towards lower diffraction angles ( $2\theta$ ), and their integrated intensities are changing evidently, suggesting a significant change in the structure parameters with temperature.

### A. Thermal-expansion coefficient

Lattice parameters for the nc Se were determined at various temperatures according to the corresponding XRD patterns, as described in Ref. 20. Figures 2(a) and 2(b) show the

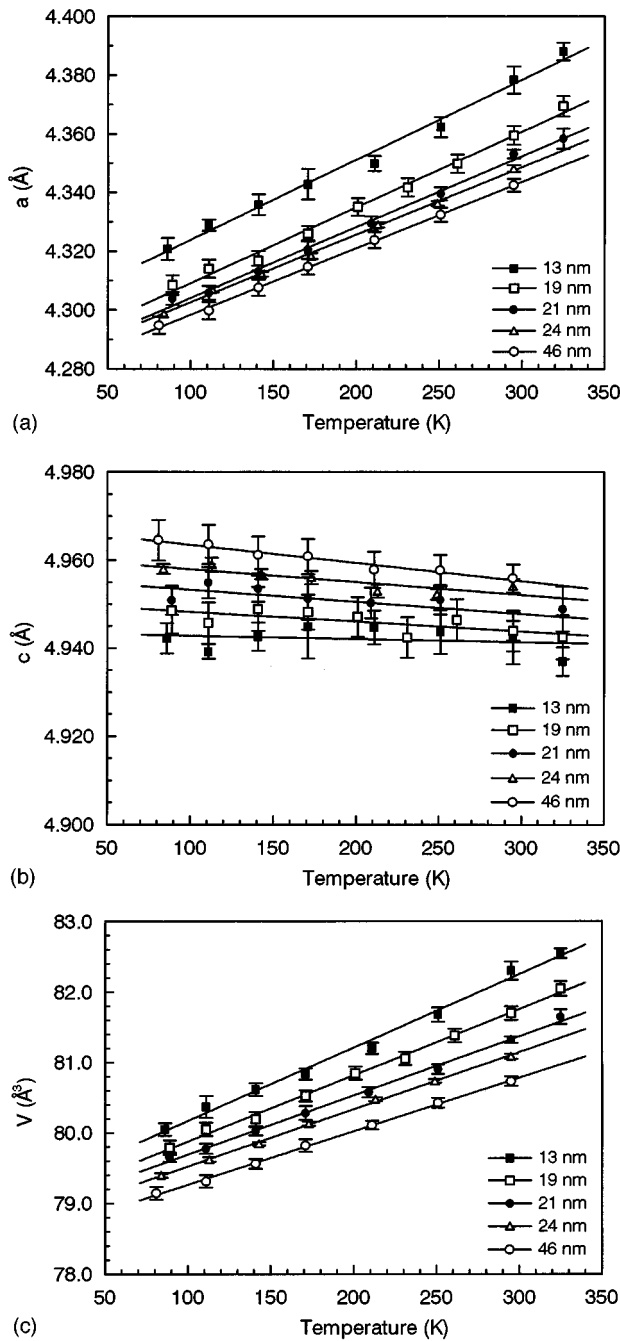


FIG. 2. Plots of the temperature dependence of the lattice parameter  $a$  (a),  $c$  (b), and the unit-cell volume (c). The solid lines are the least-square fitting to the measured data.

resultant lattice parameters  $a$  and  $c$  as a function of temperature for the nc-Se samples with different grain sizes. It is obvious that  $a$  value increases in an approximate linear relation with temperature in the measured temperature range (88–325 K). The slope of the fitting straight line (i.e., the average linear thermal-expansion coefficient (TEC) along  $a$ -axis,  $\alpha_{La}$ ) increases with a reduction of grain size. However, it is interesting to notice that  $c$  value decreases with an increasing temperature, exhibiting a contraction of the lattice along  $c$  axis, i.e., a negative linear TEC along  $c$  axis for the nc-Se specimens is obtained. Nevertheless, the unit-cell vol-

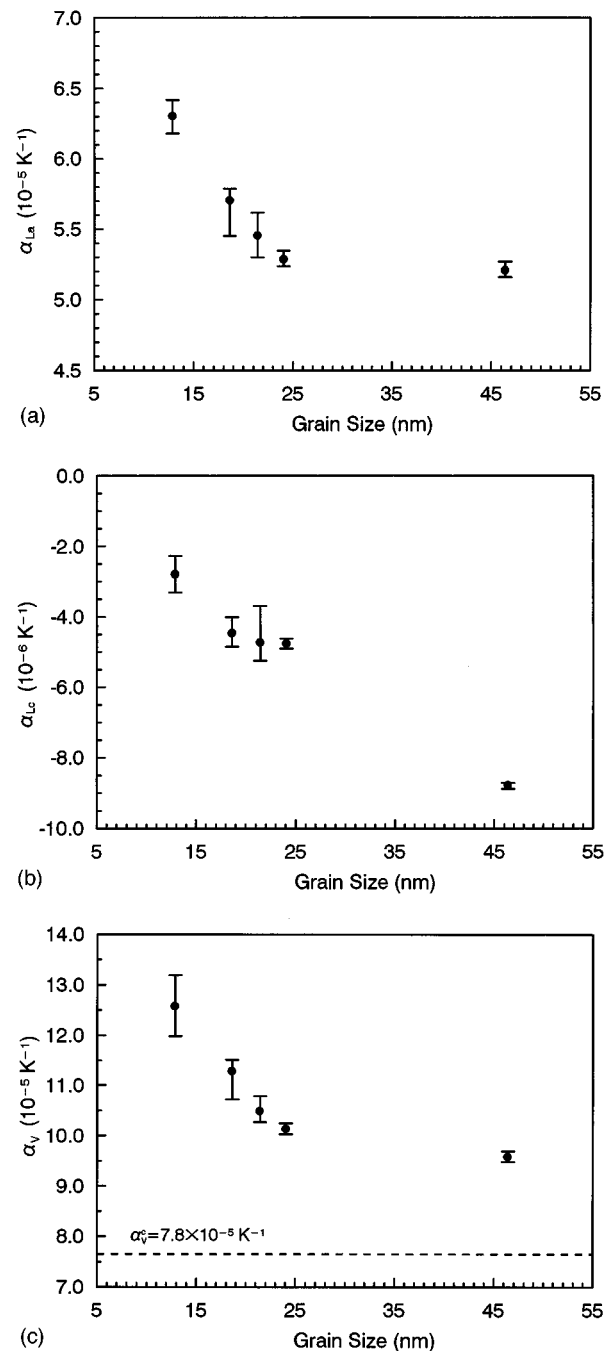


FIG. 3. Plots of the grain-size dependence of the linear TEC along the  $a$  axis (a),  $c$  axis (b), and the volume TEC (c). The dashed line is the literature value from Ref. 23.

ume  $V = [(\sqrt{3}/2)a^2c]$ , which was calculated according to the measured  $a$  and  $c$ , expands at higher temperatures, as shown in Fig. 2(c).

The average TECs for  $a$ ,  $c$ , and  $V$  within the measured temperature range were determined, as shown in Figs. 3(a)–3(c). Repeated measurements and calculation of the lattice parameters and the unit-cell volume yielded rather small scatters in the resultant data for the lattice parameters and the TECs. It is seen that with a reduction of the mean grain size from about 46 to 13 nm, the TECs increase monotonically,  $\alpha_{La}$  increases by about 21% and about 31% for  $\alpha_V$ , the TEC along  $c$  axis,  $\alpha_{Lc}$ , also increases from  $(-8.8 \pm 0.1)$

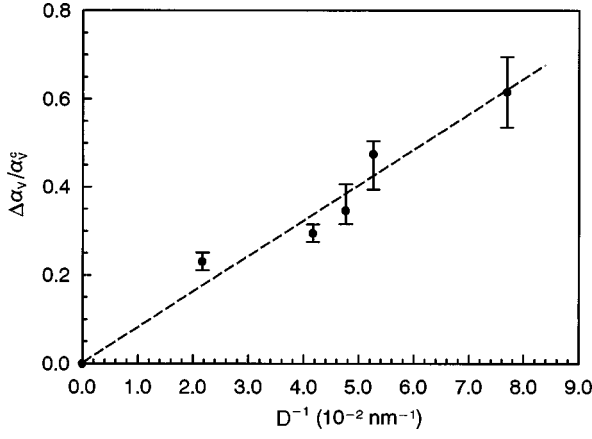


FIG. 4. A plot of the volume TEC variation  $[(\alpha_V^{nc} - \alpha_V^c)/\alpha_V^c]$  with  $D^{-1}$ .

$\times 10^{-6} \text{ K}^{-1}$  (46 nm) to  $(-2.8 \pm 0.3) \times 10^{-6} \text{ K}^{-1}$  (13 nm). Dilatometric measurements showed that the mean linear TEC is about  $2.6 \times 10^{-5} \text{ K}^{-1}$  at 300 K (the volume TEC is approximated to be  $7.8 \times 10^{-5} \text{ K}^{-1}$ ) for the conventional polycrystalline Se.<sup>23</sup> It is evident that the determined volume TECs for nc Se are larger than that for the coarse-grained Se.

The enhanced TEC of nc materials is usually attributed to the increased grain-boundary component in the nanostructures.<sup>24,7</sup> The TEC can be estimated by appropriate scaling of the grain-boundary contribution. Assuming both the grain boundary and the crystallites have the same chemical composition and elastic modulus,<sup>25</sup> one may get  $\alpha^{nc}$  of a nc sample by an approximation of

$$\alpha^{nc} = F_{gb} \alpha^{gb} + (1 - F_{gb}) \alpha^c, \quad (6)$$

where  $F_{gb}$  is the volume fraction of grain boundary that is a function of the grain size  $F_{gb} = 3\delta/D$  ( $\delta$  is a constant relative to the grain-boundary thickness),  $\alpha^{gb}$  and  $\alpha^c$  are thermal-expansion coefficients for the grain boundary and the crystallite, respectively.

Normally, the structure of both the grain boundary and the crystallites in nc materials is considered to remain unchanged when the grain size varies, i.e., both  $\alpha^{gb}$  and  $\alpha^c$  should be independent on grain size, we may get

$$\Delta\alpha = \alpha^{nc} - \alpha^c = (\alpha^{gb} - \alpha^c) \delta/D. \quad (7)$$

Taking  $\alpha_V^c = 7.8 \times 10^{-5} \text{ K}^{-1}$  for the coarse-grained Se crystal,<sup>23</sup> one may plot  $(\alpha_V^{nc} - \alpha_V^c)/\alpha_V^c$  against  $D^{-1}$ , which should yield a straight line, as shown in Fig. 4. A good straight line fitting the plot of  $(\alpha_V^{nc} - \alpha_V^c)/\alpha_V^c$  vs  $D^{-1}$  implies that the volume TEC is strongly dependent on grain size and the volume TEC enhancement follows the  $D^{-1}$  rule for the nc-Se samples.

### B. Debye-Waller parameters and the characteristic temperatures

According to Eq. (3), we plotted  $\ln[I_{obs}(hkl)/I_{cal}(hkl)]$  against  $\tau^2$  ( $\tau = 4\pi \sin\theta/\lambda$ ) for the five nc-Se samples at different temperatures in order to obtain the temperature dependence of the DWP,  $\bar{B}(T)$ . Figure 5(a) shows the plots for different nc-Se samples at 293 K and Fig. 5(b) shows the

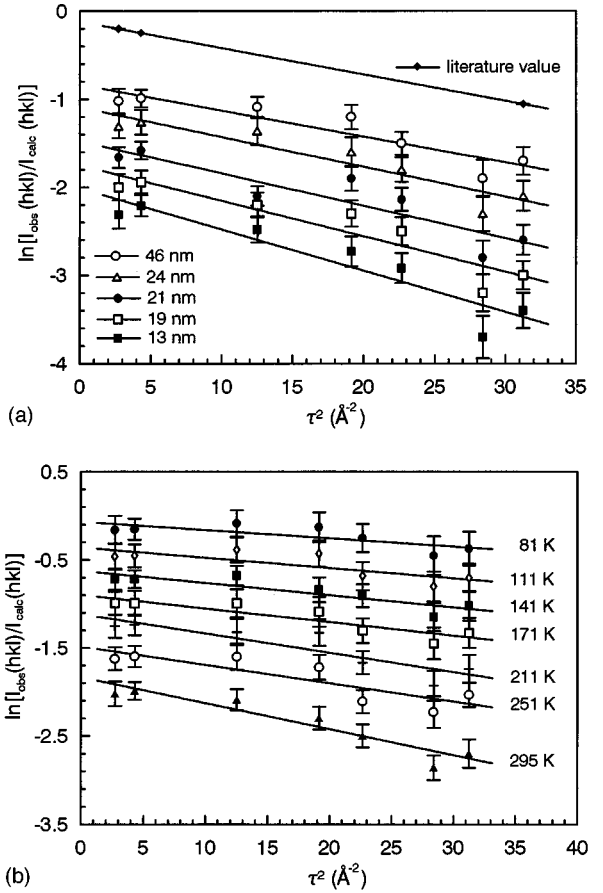


FIG. 5. (a) The logarithm of integrated peak intensities derived by the calculated intensities for the nc-Se samples with different grain sizes at 293 K. The least-square fitting is used to the measured data. The DWP can be obtained from the slope of the solid line. (b) The logarithm of integrated peak intensities derived by the calculated intensities for the nc-Se sample with a grain size of 46 nm at different temperatures.

plots of sample *E* at different temperatures. For each set of data, a straight line can be drawn (by the least-square fitting), from which the  $\bar{B}(T)$  value is obtained. From Fig. 5(a), one may see that with an increase of grain size, the absolute value of the slope for the fitting straight line decreases, i.e., the  $\bar{B}(T)$  value decreases. For sample *E*,  $\bar{B}(293) = 2.6 \pm 0.2 \text{ \AA}^2$ , which is comparable to the data for the conventional coarse-grained polycrystalline Se reported in the literature [ $\bar{B}^c(293) = 2.35 \text{ \AA}^2$ ],<sup>26</sup> as indicated in Fig. 5(a). From Fig. 5(b), one may see that  $\bar{B}(T)$  values increase remarkably at higher temperatures.

Figure 6(a) shows the temperature dependence of  $\bar{B}(T)$  for different nc-Se samples. It is clear that  $\bar{B}(T)$  varies significantly with the grain size and the temperature. With an increase of grain size, the  $\bar{B}(T)$  value shifts downwards and tends to that for the coarse-grained crystalline Se<sup>26</sup> (as reported in the literature). In terms of Eq. (5), the temperature dependence of  $\bar{B}(T)$  can be fitted by adjusting two parameters,  $\Theta_D$  and  $\bar{B}_S$ . The solid lines in Fig. 6(a) show the least-square fitting results to the measured data, and the dashed line shows the fitting results to the literature data.<sup>26</sup> The parameters  $\Theta_D$  and  $\bar{B}_S$  from the fitting results are listed

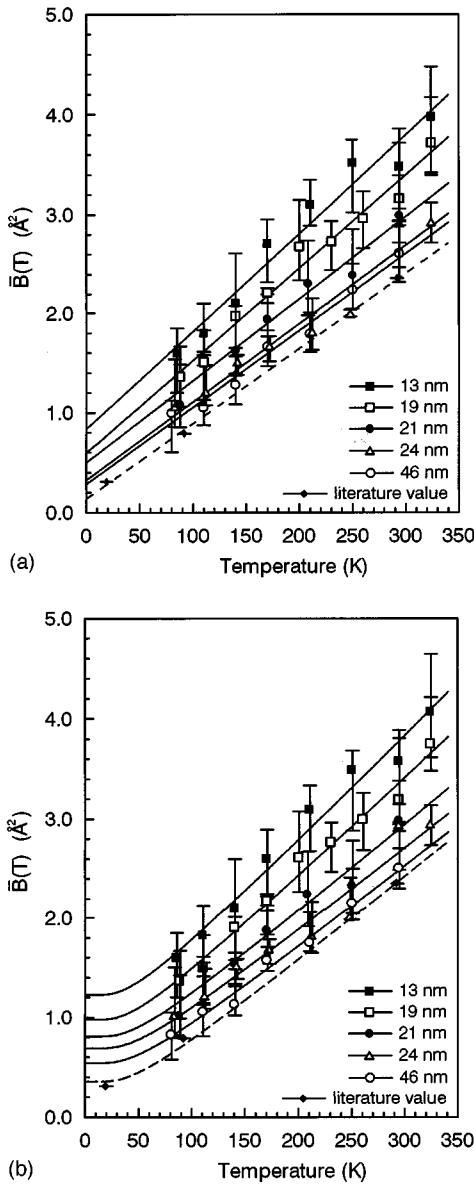


FIG. 6. The average DWP  $\bar{B}(T)$  is plotted against temperature for different nc-Se samples. The solid lines are the Debye model (a) and Einstein approximation (b) fitting of the measured data, and the dashed line represents the line fitting the literature data in Ref. 26.

in Table II. One may find that both parameters ( $\Theta_D$  and  $\bar{B}_S$ ) vary evidently with the grain size. The value of  $\bar{B}_S$  is found to decrease evidently with an increase of grain size, from  $0.77 \pm 0.2 \text{ \AA}^2$  ( $D=13 \text{ nm}$ ) to  $0.14 \pm 0.1 \text{ \AA}^2$  ( $D=46 \text{ nm}$ ), which is close to the value of  $0.08 \text{ \AA}^2$  obtained by fitting the literature  $\bar{B}(T)$  values for crystal Se.<sup>26</sup> As the mean DWP  $\bar{B}(T)$  is composed of  $\bar{B}_S$  and  $\bar{B}_T$ , we derived  $\bar{B}_{293}$  (at 293 K) based on the measured data of  $\bar{B}(293)$  and  $\bar{B}_S$ . The grain-size dependencies of  $\bar{B}(293)$ ,  $\bar{B}_S$ , and  $\bar{B}_{293}$  are shown in Fig. 7. It is seen that  $\bar{B}_{293}$  also decreases with an increasing grain size, from  $2.8 \pm 0.3 \text{ \AA}^2$  ( $D=13 \text{ nm}$ ) to  $2.5 \pm 0.2 \text{ \AA}^2$  ( $D=46 \text{ nm}$ ), but the attitude of variation of  $\bar{B}_{293}$  is smaller in comparison with that of  $\bar{B}_S$ . That means, the observed  $\bar{B}(T)$  enhancement in nc-Se samples can be mainly attributed to the enhanced static DWP ( $\bar{B}_S$ ).

TABLE II. A list of the static DWP and the Debye temperature for the nc-Se samples, which were derived from the data fitting of the temperature dependence of the mean DWP  $\bar{B}(T)$  according to Eq. (5).

Sample	Static DWP, $\bar{B}_S$ ( $\text{\AA}^2$ )	Debye temperature, $\Theta_D$ (K)
A	$0.77 \pm 0.15$	$118.8 \pm 2.1$
B	$0.53 \pm 0.10$	$122.1 \pm 2.0$
C	$0.44 \pm 0.13$	$130.0 \pm 1.6$
D	$0.27 \pm 0.12$	$133.1 \pm 1.7$
E	$0.14 \pm 0.08$	$134.0 \pm 1.4$
F <sup>a</sup>	0.08	135.9

<sup>a</sup>The value fitted from the literature value in Ref. 26.

The enhancement of static DWP ( $\bar{B}_S$ ) in nc materials is normally attributed to the increase of volume fraction of grain boundary.<sup>10</sup> According to the simple two-state model,<sup>10</sup> one may describe the overall static DWP of a nc sample by

$$\bar{B}_S^{\text{nc}} = F_{\text{gb}} \bar{B}_S^{\text{gb}} + (1 - F_{\text{gb}}) \bar{B}_S^{\text{c}}, \quad (8)$$

where  $F_{\text{gb}}$  is the volume fraction of grain boundaries which is proportional to  $1/D$ , and  $\bar{B}_S^{\text{gb}}$  and  $\bar{B}_S^{\text{c}}$  are the static DWPs for the grain boundary and the crystallite, respectively. Then the  $\bar{B}_S^{\text{nc}}$  enhancement relative to  $\bar{B}_S^{\text{c}}$ ,  $\Delta \bar{B}_S / \bar{B}_S^{\text{c}} = (\bar{B}_S^{\text{nc}} - \bar{B}_S^{\text{c}}) / \bar{B}_S^{\text{c}}$ , should be proportional to  $1/D$ . A plot of the enhancement of  $\bar{B}_S^{\text{nc}}$  vs  $1/D$  for the nc-Se sample, can be well fitted by a straight line, as shown in Fig. 8. This result is rather similar to the observation in nc Cr made by consolidation of UFPs, implying that the simple two-state model could be used to describe the grain-size dependence of the static DWP of nc element Se. Alternatively, from a thermodynamic point view, the enhancement of  $\bar{B}_S$  in the nc-Se samples with smaller grains can also be explained by means of the larger defects solubility caused by the increase of the Gibbs free energy from the interfaces.<sup>27</sup>

An enhancement in the static DWP means larger displacements of atoms from their equilibrium lattice locations. Comparative investigations indicated that ultrafine metal powders [Cr (Ref. 10), Pd (Refs. 12 and 13), Au (Refs. 14 and 15) and Pb (Ref. 16)] possess a larger static DWP than

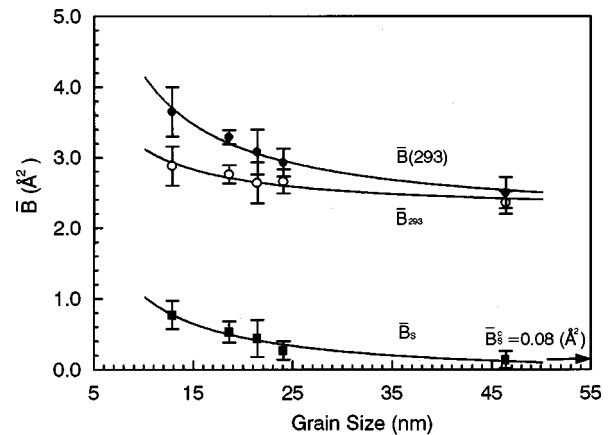


FIG. 7. Plots of the mean DWP, the static and the thermal DWP at 293 K fitted from Debye model vs the mean grain size.

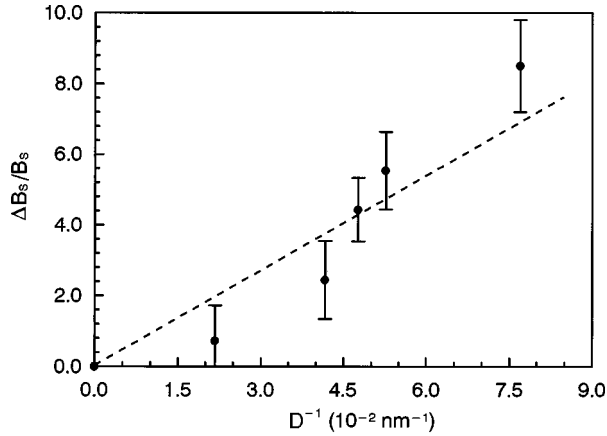


FIG. 8. A plot of the static atomic displacement change  $[(\bar{B}_S^{nc} - \bar{B}_S^c)/\bar{B}_S^c]$  versus  $D^{-1}$ .

the corresponding bulk crystals. Ohshima and co-workers<sup>15</sup> determined the DWP for the inert-gas condensed ultrafine Au powders over a temperature range 112–298 K. They found a rather small increase in the thermal component of DWP compared with that for the bulk crystalline Au, while the static component increases significantly, which is sensitive to the synthesis conditions. For a nc Pd consolidated from UFPs, Eastman and co-workers<sup>8</sup> found that an increase in the static displacements plays a dominant role in the enhancement of the mean DWP as the thermal component is essentially unchanged. These results, as well as the observations in the nc element Se in the present work, suggest that the static atomic displacements might dominate the enhancement of DWP for nc materials.

Figure 9 shows the Debye characteristic temperature for the nc-Se samples as a function of grain size obtained from the data fitting of the temperature dependence of  $\bar{B}(T)$ . With a decrease of the mean grain size from 46 to 13 nm, the Debye characteristic temperature drops from  $134 \pm 1$  to  $119 \pm 2$  K. These values are smaller than that obtained by fitting the literature value for Se crystal ( $\Theta_D^c = 136$  K),<sup>26</sup> and the tabulated Debye temperature (135 K).<sup>26</sup> The  $\Theta_D$  values for

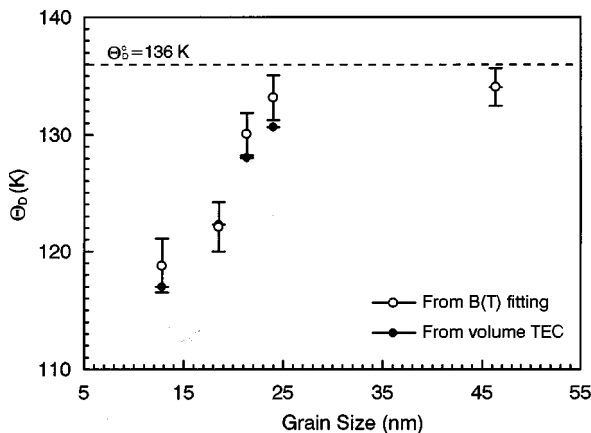


FIG. 9. Plots of the Debye characteristic temperature (that was obtained from the fitting of the temperature dependence of  $\bar{B}(T)$ , open circles) and the Debye characteristic temperature (that was derived from the measured volume TEC values, solid circles) against the mean grain size.

the nc Se with larger grains (24 and 46 nm) are close to  $\Theta_D^c$ , indicating that the fitting results of the  $\bar{B}(T) \sim T$  dependence by means of the Debye approximation may yield fairly consistent results for the Debye temperature.

From Lindemann's equation<sup>28</sup> and Grüneisen's theory of the solid state,<sup>23</sup> the Debye temperature is related to the volume thermal-expansion coefficient by

$$\Theta_D = c / \sqrt{\alpha_V V^{2/3} A_r}, \quad (9)$$

where  $c$ ,  $A_r$ , and  $V$  are a constant, atomic weight compared to  $C^{12}$  and the mole volume of Se, respectively. According to this relation, one may estimate the  $\Theta_D$  value from the measured volume TEC data. The estimated Debye temperature from the measured volume TEC data is also displayed in Fig. 9. It is obvious that these sets of data are consistent with that from the fitting of the DWPs. The coincidence of these two sets of characteristic temperature data, that derived from two independent approaches, indicated an intrinsic feature of the nc Se that the characteristic temperature is considerably depressed related to that for the coarse-grained polycrystalline Se and it decreases with a reduction of grain size.

For the nc materials, it is considered that the Debye model might not be applicable as the long-wavelength acoustic vibration may not exist anymore.<sup>15</sup> Supposing the ultrafine crystallite as an assembly of atoms, each of which is oscillating independently with a certain frequency  $\gamma_E$ , one may use the Einstein approximation for the lattice vibrations

$$B_T = \frac{6h^2}{mk_B \Theta_E} \left[ \frac{1}{\exp(\Theta_E/T) - 1} + \frac{1}{2} \right], \quad (10)$$

where  $m$ ,  $T$ ,  $h$ , and  $k_B$  are the atomic mass, the temperature, the Planck's constant, and the Boltzmann constant, respectively, and  $\Theta_E$  is the Einstein characteristic temperature defined by  $h\gamma_E = k_B \Theta_E$ . The Einstein approximation is also normally applicable to cubic crystals, however, for the hexagonal structure of Se as in the present case, we utilized it as an approximation because of no existing model available for the hexagonal structure. According to Eqs. (4) and (10), the Einstein temperature  $\Theta_E$  and static DWP  $\bar{B}_S$  can be obtained by fitting  $\bar{B}(T)$  values at several temperatures, as shown in Fig. 6(b). The curves in the figure give different Einstein temperatures and static DWPs for different nc-Se samples, as shown in Table III. Compared to Table II, it is clear that the Einstein temperature is slightly smaller (about 2 K) than the Debye temperature for each nc-Se sample, and the static DWP data fitted from Einstein approximation is about  $0.1 \text{ \AA}^2$  smaller than that from Debye model. From the comparison of the two sets of data, one can see that the Debye model can also be applied to the present system. In fact, the nc-Se systems are composed of fairly large grains, i.e., 10 nm grains have lots of atoms and the long-wavelength acoustic vibration still exists. Moreover, the long-wavelength phonon models have been observed on surfaces thin films, and the density of states of a nc Ni was not found to be very different from that of the bulk materials.<sup>29</sup>

The depressed Debye temperatures in nanometer-sized metallic powders have been detected in several systems. The Debye temperature for ultrafine silver particles with a mean

TABLE III. A list of the static DWP and the Einstein characteristic temperature for the nc-Se samples, which were derived from the data fitting of the temperature dependence of the mean DWP  $\bar{B}(T)$  according to Eqs. (4) and (10).

Sample	Static DWP, $\bar{B}_S$ ( $\text{\AA}^2$ )	Einstein characteristic temperature, $\Theta_E$ (K)
A	$0.67 \pm 0.21$	$116.9 \pm 3.3$
B	$0.43 \pm 0.18$	$120.6 \pm 2.8$
C	$0.33 \pm 0.17$	$127.9 \pm 1.3$
D	$0.16 \pm 0.20$	$131.3 \pm 2.8$
E	$0.03 \pm 0.16$	$132.2 \pm 1.5$
F <sup>a</sup>	-0.20	134

<sup>a</sup>The value fitted from the literature value in Ref. 26.

size of 15 nm was reported to be 156 K, which is 25% less than the bulk value ( $\Theta_D = 212$  K).<sup>17</sup> A reduced Einstein characteristic temperature of about 15% was observed in 10 nm gold particles compared to that for the bulk crystal ( $\Theta_D = 168$  K).<sup>15</sup> For nc materials assembled by UFPs, comparable or depressed Debye temperatures were also reported in Pd (Ref. 8) and Sn (Ref. 18). A 20% depression in the Debye temperature was also observed in the porosity-free nc Cu made by severe plastic deformation.<sup>30</sup> The observed depression in the characteristic temperature in the nc Se is in agreement with the results reported in the literature.

The characteristic temperature of material is a fundamentally physical parameter designating the cohesion of atoms. The higher characteristic temperature indicates a stronger cohesion of atoms in the material. The depression of characteristic temperature in the nc Se implies a decrease in the cohesion of atoms in the nm-sized crystallites, which agrees well with the measured grain-size dependence of the DWP. With a reduction of grain size, the atomic displacement from their ideal lattice locations increases, which may weaken the cohesion between neighboring atoms. In fact, the observed larger thermal and static component of DWP in nc-Se samples with smaller grains may result in a decrease in the elastic modules and hence a depression of the effective characteristic temperature. Thermodynamic calculations indicated that the TEC increases remarkably with an increase of the excess volume of the lattice,<sup>31</sup> which is closely related to the static displacements of atoms. Larger static atomic displacements from the ideal lattice positions may result in an increase in the effective excess volume of the lattice. Actually, the dilated lattice in the nc Se with smaller grains has been experimentally observed in our previous paper.<sup>20</sup>

Therefore, one may see that the measured thermal properties and their grain-size dependence of nc-Se samples agree well with each other, and are also consistent with the structure characteristics of the nc-Se materials.<sup>20</sup> The increases of the unit-cell volume,<sup>20</sup> microstrain,<sup>20</sup> volume TEC, and the static component of the DWP with a reduction of grain size

is found to follow the simple  $D^{-1}$  rule. This behavior could be explained in terms of the simple two-state model for the nc materials.<sup>10</sup> In the two-state model, it is supposed that two discrete regions with differing microstructures (e.g., concentrations of defects) and properties coexist. Although the above-mentioned structure and properties can be scaled by the  $D^{-1}$  relation, it is not necessarily true for the nc material to possess this extremely simple structure. In reality, a continuous distribution of differing microstructure (or defects) and properties exist in the nm-sized crystallites and grain boundaries. Localization of all defects on the grain boundaries is a simple approximation of the real nanostructure. To uncover the intrinsic nature of the microstructure and properties of nc materials, a systematic investigation on nc materials with a wide grain-size range (especially with smaller grains, say less than 10 nm) would be valuable.

#### IV. CONCLUSIONS

Porosity-free bulk nanocrystalline hexagonal elemental selenium with grain sizes ranging from 13 to 46 nm made by crystallizing melt-quenched amorphous Se solid have been investigated by means of quantitative x-ray-diffraction analysis in a temperature range of 88–325 K.

With an increase of temperature, lattice parameter  $a$  increases but  $c$  decreases, exhibiting different thermal-expansion behaviors along different crystallography directions. With a reduction of grain size, the linear TECs (both along  $a$  axis and  $c$  axis) increase significantly, resulting in a significant increase in the volume TEC. The enhancement of the volume TEC for the nc-Se samples increases with a reduction of grain size and follows the  $D^{-1}$  rule.

The temperature dependence of the mean DWP was measured, from which the static and thermal components of the DWP, as well as the characteristic temperatures for the nc-Se samples were obtained. The observed enhancement in the mean DWP can be attributed mainly to an increase of the static atomic displacement with a reduction of grain size that follows the  $D^{-1}$  rule. The thermal DWP increases slightly with decreasing the mean grain size. The Debye temperature for the nc-Se specimens was found to decrease from 134 to 119 K when the mean grain size drops 46 to 13 nm. These results suggests larger displacements of the atoms from their ideal lattice locations and more defects in the nc-Se samples with smaller grains. The thermal properties and their grain-size dependence of nc elemental Se samples agree well with the characteristic microstructures revealed by XRD experiments.

#### ACKNOWLEDGMENTS

This work was financially supported by the National Science Foundation of China and the Chinese Academy of Sciences (Grant Nos. 59625101 and 59431021).

\*Corresponding author. Fax: +86-24-3891 320; Tel: +86-24-3843 531; Electronic address: kelu@imr.ac.cn

<sup>1</sup>J. Rupp and R. Birringer, Phys. Rev. B **36**, 7888 (1987).

<sup>2</sup>E. Hellstern, H. J. Fecht, F. Zhu, and W. L. Johnson, J. Appl. Phys. **65**, 305 (1989).

<sup>3</sup>K. Lu, R. Lück, and B. Predel, Z. Metallkd. **84**, 740 (1993).

<sup>4</sup>N. X. Sun and K. Lu, Phys. Rev. B **54**, 6058 (1996).

<sup>5</sup>U. Erb (private communication).

<sup>6</sup>H. Y. Tong, J. T. Wang, B. Z. Ding, H. G. Jiang, and K. Lu, J. Non-Cryst. Solids **150**, 444 (1992).

- <sup>7</sup>R. Birringer and H. Gleiter, in *Advance in Materials Science, Encyclopedia of Materials Science and Engineering*, edited by R. W. Cahn (Pergamon, Oxford, 1988), p. 339.
- <sup>8</sup>J. A. Eastman, M. R. Fitzsimmons, and L. J. Thompson, *Philos. Mag. B* **66**, 667 (1992).
- <sup>9</sup>K. Lu and M. L. Sui, *Acta Metall. Mater.* **43**, 3325 (1995).
- <sup>10</sup>J. A. Eastman and M. R. Fitzsimmons, *J. Appl. Phys.* **77**, 522 (1995).
- <sup>11</sup>M. R. Fitzsimmons, J. A. Eastman, M. Müller-Stach, and G. Wallner, *Phys. Rev. B* **44**, 2452 (1991).
- <sup>12</sup>K. Ohshima, S. Yatsuya, and J. Harada, *J. Phys. Soc. Jpn.* **50**, 3071 (1981).
- <sup>13</sup>M. Minagaki, Y. Sasaki, and M. Sakai, *J. Mater. Sci.* **18**, 1803 (1983).
- <sup>14</sup>J. Harada, S. Yao, and A. Ichimiya, *J. Phys. Soc. Jpn.* **48**, 1625 (1980).
- <sup>15</sup>K. Ohshima, S. Yatsuya, and J. Harada, *J. Phys. Soc. Jpn.* **48**, 1631 (1980).
- <sup>16</sup>V. Novotny, T. M. Holden, and G. Dolling, *Can. J. Phys.* **52**, 748 (1974).
- <sup>17</sup>Y. Kashiwase, I. Nishida, Y. Kainuma, and K. Kimoto, *J. Phys. C* **38**, C2-57 (1977).
- <sup>18</sup>L. B. Hong, C. C. Ahn, and B. Fultz, *J. Mater. Res.* **10**, 2408 (1995).
- <sup>19</sup>J. Jiang, S. Ramasamy, R. Birringer, U. Gonser, and H. Gleiter, *Solid State Commun.* **80**, 525 (1991).
- <sup>20</sup>Y. H. Zhao, K. Zhang, and K. Lu, preceding paper, *Phys. Rev. B* **56**, 14 322 (1997).
- <sup>21</sup>A. Guinier, *X-ray Diffraction, in Crystals, Imperfect crystals and Amorphous Bodies* (Freeman, San Francisco, 1963).
- <sup>22</sup>B. E. Warren, *X-ray Diffraction* (Dover, New York, 1990).
- <sup>23</sup>*American Institute of Physics Handbook*, 2nd ed., edited by D. E. Gray *et al.* (McGraw-Hill, New York, 1963), p. 4–66.
- <sup>24</sup>H. J. Klam, H. Haln, and H. Gleiter, *Acta Metall.* **35**, 2101 (1987).
- <sup>25</sup>K. Lu, H. Y. Zhang, Y. Zhong, and H. J. Fecht, *J. Mater. Res.* **12**, 923 (1997).
- <sup>26</sup>*International Tables for X-ray Crystallography III*, edited by C. H. Macgillavry and G. D. Rieck (Reidel, Dordrecht, 1983), p. 239.
- <sup>27</sup>K. Lu and M. L. Sui, *J. Mater. Sci. Technol.* **9**, 419 (1993).
- <sup>28</sup>*Thermodynamics of Solids*, edited by R. A. Swalin (Wiley, New York, 1972).
- <sup>29</sup>S. Lehwald, J. Szeftel, H. Ibach, T. S. Rahman, and D. L. Mills, *Phys. Rev. Lett.* **50**, 518 (1983).
- <sup>30</sup>K. Zhang and K. Lu (unpublished).
- <sup>31</sup>M. Wagner, *Phys. Rev. B* **45**, 635 (1992).